Measuring 3D Wind Fields in Mountain Waves Using Sailplane Flight Data

Ni Zhang
nzh15@uclive.ac.nz

Rick Millane
rick.millane@canterbury.ac.nz

Computational Imaging Group
Department of Electrical and Computer Engineering
University of Canterbury, Private Bag 4800, Chistchurch, New Zealand

Einar Enevoldson
James Murray

NASA Dryden Flight Research Center
Edwards, California, 93523, USA

Abstract

Mountain lee waves are of considerable interest in meteorology and also are used routinely by sailplane pilots as a source of lift for high-attitude and long-distance flights. Data collected during wave flights therefore are potentially useful for studying the structure of mountain waves. Novel methods are described for determining three-dimensional wind velocities in mountain waves using limited data from sailplane flights. Results are presented for application of the methods to data from a flight in the Sierra Nevada mountain wave.

Presented at the XXX OSTIV Congress, Szeged, Hungary, 28 July – 4 August 2010

Nomenclature

$\mathbf{v}_g$	ground velocity of the sailplane
$\mathbf{v}_a$	velocity of the sailplane relative to the airmass
$\mathbf{v}_w$	wind velocity
v_a	airspeed
v_{vw}	vertical wind speed
v_{vg}	vertical speed of the sailplane
v_s	sailplane sink rate
v_e	vertical speed component of the sailplane due to energy exchange

Introduction

Mountain lee waves provide a common source of lift for sailplane pilots. In appropriate geographical and meteorological conditions, lee wave systems can exist over a large area and to high altitudes. Sailplane flights in these systems also can cover large distances and altitudes. Mountain waves are a form of atmospheric gravity wave that is generated by flow over elevated terrain in a stable, stratified atmosphere [1]. Mountain waves used by sailplane pilots are generally trapped or resonant waves that form in atmospheric waveguides and propagate horizontally [2]. Wavelengths are typically about 2-10 km and they can extend far downwind of the mountain. Aside from their use by sailplane pilots, mountain waves are of significant importance in meteorology. They can influence the vertical structure of the wind speed and temperature fields and can affect ozone concentration [3, 4]. Momentum dissipation associated with mountain waves results in drag that affects the general circulation of the atmosphere [5]. Mountain waves also can produce strong downdrafts that can be an aviation hazard [6]. They also play a role in the vertical transport of aerosols and trace gases.

Despite their importance, measurement of the three-dimensional wind field in mountain wave systems is not without difficulty. Radiosondes give information on the horizontal windspeed and direction but only over the radiosonde ascent path. The vertical wind speed also can be estimated from radiosonde flights by correcting for the balloon ascent rate, but this is error-sensitive. Doppler radar is a versatile technique for remote measurement of 3D wind fields, but the equipment required is large and expensive [7].

Another avenue for measuring winds in the atmosphere is using aircraft flight data. Indeed, the flight systems of transport aircraft make routine, real-time estimates of the horizontal wind speed and direction. Such aircraft do not generally fly in mountain waves, however. Specialised research aircraft and light aircraft flight data have been used for atmospheric research but these also use sophisticated and expensive instrumentation [8,9]. Since sailplanes are often flown in mountain wave systems, there is a potential to use recorded flight data to derive the wind velocities along the flight path. With an appropriate wave flight, quite comprehensive information potentially could be obtained. In fact, some of the earliest information on mountain waves was obtained from sailplane flights [10]. There are two approaches to this problem. One is to install in a sailplane a sophisticated flight measurement system that records sufficient data to make a direct measurement of the wind speed and direction. Such a system has been described for a sailplane that uses airspeed, acceleration, altitude, heading, position, and control surface deflection data to derive wind speed and direction [11]. This is

an expensive approach, however, and would be limited to only a few sailplanes. The second option is to develop methods that can use the limited data recorded from conventional sailplane flight recorders that are often installed in gliders. Such an approach offers the possibility of analysing data from many sailplane flights, and is the option considered here.

Modern sailplane flight computers generally calculate estimates of the wind speed and direction, and the vertical wind speed (lift). There are, however, a number of limitations with using these instruments for accurate data collection for postflight analysis. The wind speed and direction estimates are generally based on circling flight but the precision when the pilot is not executing a constant rate turn is unclear. Estimates also may be made for a dogleg in the flight path but the precision of the estimates obtained in this case is not clear. Estimates of lift (vertical wind speed) are generally based on data from a total energy or Netto variometer. The precision obtained is dependent on the kind of the total energy correction used and the time constants of the instrument. Furthermore, estimates of wind speed and direction and lift are made in real time and displayed to the pilot, but are usually not logged in the instrument and so are not available for later analysis. Any data (aside from position) that is recorded, is usually stored only in summary (statistical) form.

The use of sailplane data for analyzing mountain waves is not new. A number of early studies were qualitative in nature [10]. More recently, the OSTIV Mountain Wave Project has collected data from a well-instrumented sailplane and results have been presented for lee waves in the Andes [12]. Flight data from multiple flights also have been analysed to derive statistical characteristics of lee waves in northern Germany [13]. Flights in a sailplane fitted with a digital variometer and a gyroscope/accelerometer also have been used to study internal rotor structures [14]. Our objective here is to supplement these studies by developing algorithms to process basic sailplane flight data to obtain rigorous estimates of the 3D wind field in mountain waves using routine flights and a sailplane equipped with minimal instrumentation.

In the next section we analyse the general problem of determining a 3D wind field from limited flight data. In the following section we summarize an algorithm that we recently have developed (described in detail in Ref. 15) that uses logs of GPS position and airspeed to estimate the 3D wind velocity in mountain waves. An application of the method to data from a flight in lee waves of the Sierra Nevada (also described in Ref. 15) is presented in the next section. Additional results are presented concerning the accuracy of various components of the algorithm. Concluding remarks are made in the final section.

Wind fields from limited flight data

Consider the general problem of determining a 3D wind field from limited aircraft flight data. Since we are interested in (the laminar portion of) mountain waves, we assume that the horizontal component of the wind field varies slowly in space and time. What we mean here, approximately, is that the horizontal component is expected to be relatively constant over horizontal distances of the order of 5 km, over vertical distances of the order of 100 m, and over time intervals on the order of 10 minutes. These restrictions are expected to usually apply in stable, high altitude mountain lee waves. These assumptions allow a single estimate of the wind velocity to be made using data collected in spatio-temporal regions of a size limited by these values. It is convenient to analyze the horizontal and vertical components of the wind velocity separately. This separation involves making some minor assumptions of little significance. Estimation of the horizontal and vertical wind velocities are described in the following two subsections.

Horizontal wind velocity

The objective here is to estimate the horizontal component of the wind velocity (i.e. the speed and direction) from limited onboard flight data. The fundamental relationship used is that the ground (inertial) velocity of the sailplane, $\mathbf{v}_g$, is the vector sum of the velocity of the sailplane relative to the airmass, $\mathbf{v}_a$, (i.e. its airspeed and heading) and the wind velocity, $\mathbf{v}_w$, i.e.

$$\mathbf{v}_g = \mathbf{v}_a + \mathbf{v}_w \tag{1}$$

as shown in Fig. 1. If the ground velocity, airspeed and heading are measured, then it is straightforward to calculate the wind velocity using Eq. 1. This calculation is made on flight systems in commercial aircraft using GPS position, airspeed and compass data. All of this data are not available from the usual sailplane instrumentation, however. Ground velocity data is generally available, airspeed data may sometimes be available, but heading data are generally not recorded or logged.

Since most sailplanes use pitot-static airspeed indicator based on impact pressure, for high altitude flight, an important consideration is the conversion of the measured indicated (or calibrated) airspeed (IAS) to true airspeed (TAS). If the altitude is not too high, the incompressible approximation applies and the IAS, denoted $v_a{}^I$, needs be corrected only for air density and the

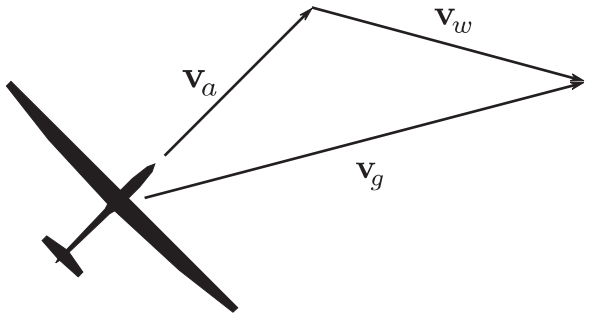

Figure 1 The aircraft ground velocity $\mathbf{v}_g$ is the vector sum of the aircraft velocity relative to the airmass $\mathbf{v}_a$ and the wind velocity $\mathbf{v}_w$.

TAS, v_a, is given by

$$v_a = v_a{}^I \left(\frac{T}{T_0} \frac{P_0}{P} \right)^{1/2} \tag{2}$$

where T and P are the temperature and pressure at altitude and T_0 and P_0 are reference (usually sea-level) values. This correction is made based either on onboard measurements of temperature and pressure, or estimates of these based on standard atmosphere values. The latter is generally sufficiently accurate in practice. Since wave flights can reach quite high altitudes, it is necessary to consider the effects of compressibility. It can be shown that for low Mach number M (the ratio of the TAS to the speed of sound), the airspeed corrected only for density must be multiplied by the additional factor [16]

$$x = \left[1 + \frac{1}{8} \left(1 - \frac{P}{P_0} \right) M^2 \right]^{-1} \tag{3}$$

to obtain the TAS. To quantitate the error due to ignoring compressibility, we calculate the relative error $\delta = (1-x)$ versus altitude, assuming a standard atmosphere, for two typical sailplane IAS of 30 and 50 m/s. The relative error versus altitude is shown in Fig. 2. This shows that even for relatively high IAS, the effect of compressibility is less than 2% for altitudes less than 14000 m. Therefore, only the density correction Eq. 2 is applied.

Consider first the case where the ground velocity (derived from logged GPS position) and airspeed (from logged airspeed indicator data) are available. Since the heading is unknown, there is, therefore, a one-parameter family of solutions for the wind velocity, corresponding to the tail of the wind speed vector lying on a circle with radius equal to the airspeed, as shown in Fig. 3(a). Ground speed and airspeed data alone are, therefore, insufficient to uniquely define the wind velocity. Consider now the case where two sets of measurements of the ground velocity and airspeed are made in a region where the wind velocity is constant (or almost constant), and the ground velocities are different (due to a change in $\mathbf{v}_a$). The one-parameter ambiguity for the wind velocity then reduces to a twofold ambiguity, i.e. there are only two solutions. This comes about because the two sets of measurements give two circles (as shown in Fig. 3(b)), and valid solutions, therefore, occur only where the circles intersect, which occurs at two points. If measurements are made for a multiple pairs of different ground velocities then these twofold ambiguities are resolved, giving a unique solution for the wind velocity. The geometry of the two circles described above is such that a unique solution is obtained only if the heading is different for the two sets of data [15]. Therefore, the wind velocity cannot be determined during straight flight, and an estimate becomes more accurate the more rapidly changes in heading (turning) occur. An algorithm to estimate the horizontal wind velocity based on the above approach is described in Ref. 15 and is

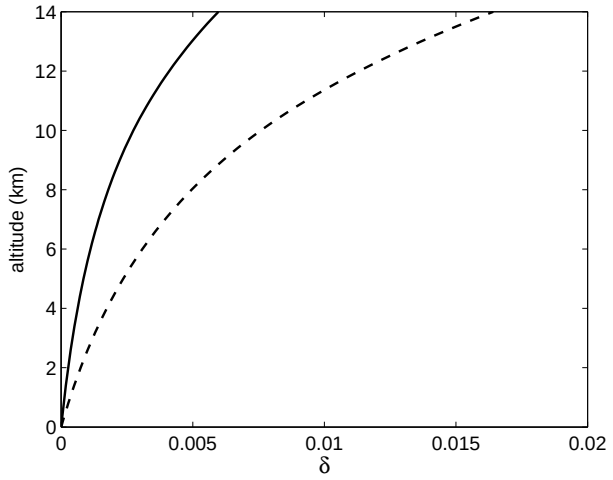

Figure 2 The relative error in the TAS due to ignoring compressibility versus altitude for two sailplane IAS of 30 m/s (solid line) and 50 m/s (dashed line).

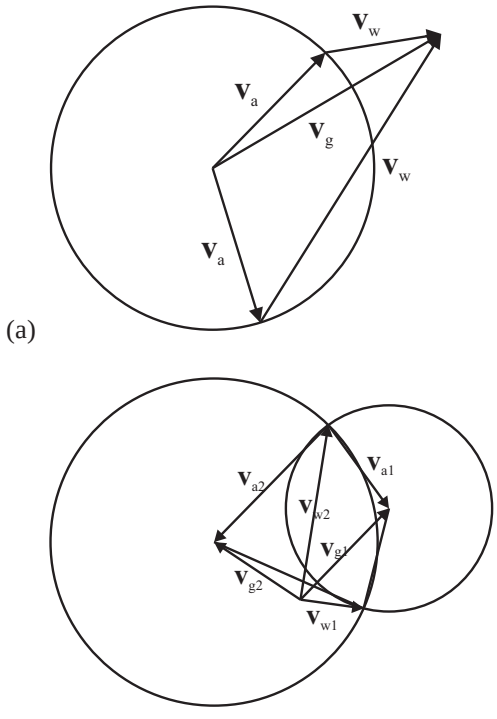

Figure 3 (a) The relationship between the air, wind and ground velocities if only the ground velocity and airspeed are known. All vectors with tails terminating on the circle are valid wind velocity solutions. There are multiple such solutions, two of which are shown. (b) The relationship as in (a) if two sets of ground velocities and airspeeds are known. The only consistent solutions for the wind velocity are where the two circles intersect. The two solutions for the air velocity and wind velocity are shown.

summarised in the next section.

Vertical wind speed

The vertical wind speed can be measured in principle by logging data from a variometer equipped with total energy correction and sink rate correction based on the particular sailplane flight polar. However, this approach presents a number of difficulties. Such a variometer may not be installed, and in any case most flight recorders do not log a corrected climb rate. Therefore, we take the approach of deriving the vertical velocity of the sailplane relative to the ground from the GPS altitude and applying appropriate corrections for the sailplane sink rate and potential/kinetic energy exchange.

Consider first the sailplane sink rate. Although the sink rate depends on the airspeed and the air density (altitude), the glide angle depends only on the IAS and is independent of the air density. This means that the sink rate at altitude, denoted v_s, is that derived from the (sea-level) polar at the given IAS, multiplied by the factor ${v_a}/{v_a}^I$ [15]. This factor is shown versus altitude in Fig. 4, calculated based on a standard atmosphere. It is seen to be significant even at modest altitudes and is, therefore, important in calculating the sink rate at altitude. Note that v_s is always negative.

A further consideration is the effect of turning on the sink rate, since the sailplane polar is based on level flight. The effect of bank on the sink rate can be estimated as follows [17]. Consider the sailplane in a turn at airspeed v_a and bank angle ϕ. The wing is operating at the same lift coefficient in level flight if the speed were $v_a \cos^{1/2}\phi$. The equivalent sink rate can then be obtained from the level-flight polar and the lift-to-drag ratio calculated. The sink rate can then be calculated, noting the vertical component of the lift is $L\cos\phi$. Putting all this together shows that the sink rate $v_s(\phi)$ at bank angle ϕ and airspeed v_a is

$$v_s(\phi) = f(v_a \cos^{1/2}\phi)\cos^{-3/2}\phi \tag{4}$$

where the function $f(v)$ is the level-flight polar of sink rate versus IAS. This effect is shown in Fig. 5 by plotting the difference in sink rate due to bank, $\Delta v_s(\phi) = -(v_s(\phi) - v_s(0))$, as a function of bank angle for two typical sailplane airspeeds using the DG-500M polar. It is seen that the effect is small for bank angles less than 30°. Even at altitude, as described above, the effect will be small. Since high bank is infrequent in wave flights, our approach is to ignore this effect, but to calculate the bank angle (this is easily done using the flight path relative to the air that can be calculated once the horizontal wind velocity has been calculated) and exclude from analysis any points at which the bank exceeds 30°.

Secondly, the effect of energy exchange when the sailplane is accelerating needs to be considered. If, for example, the sailplane airspeed is decreasing, then there is an additional climb rate due to the conversion of kinetic to potential energy of the sailplane. Equating the rates of change of potential and kinetic energy shows that the corresponding vertical speed component, v_e, is

$$v_e = -\frac{v_a}{g}\frac{dv_a}{dt} \tag{5}$$

where dv_a/dt is the rate of change of airspeed and g is the acceleration due to gravity. The vertical wind speed, denoted v_{vw}, is then calculated as

$$v_{vw} = v_{vg} - v_s - v_e \tag{6}$$

where v_{vg} is the vertical speed of the sailplane relative to the ground calculated from the GPS altitude.

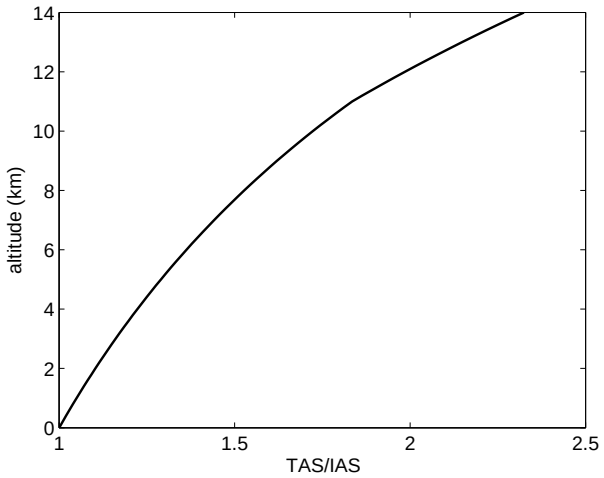

Figure 4 The correction factor for the sink rate at altitude derived from the sea-level polar, for a standard atmosphere.

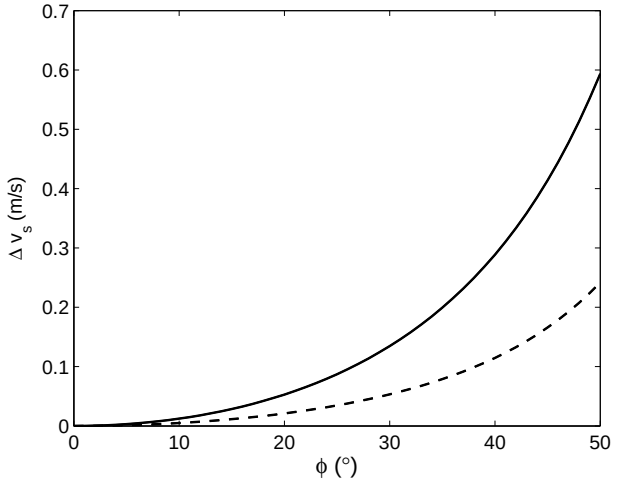

Figure 5 Error in sink rate due to banked flight at sailplane IAS of 30m/s (solid line) and 50m/s (dashed line) for the DG-505M.

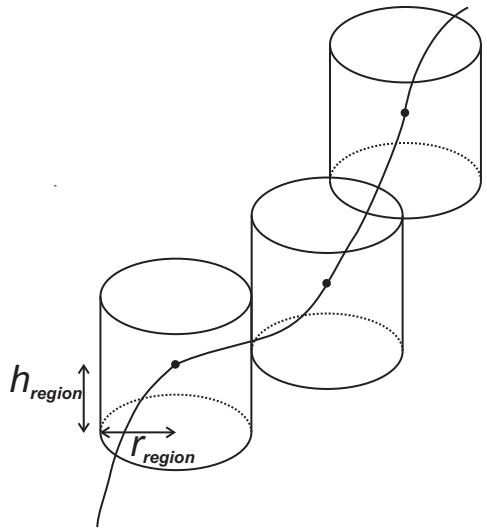

Figure 6 Partitioning of the flight path into cylindrical regions [15].

3D wind velocity from position and airspeed

As described in the previous section, the horizontal component of the wind velocity can be estimated from multiple measurements of the ground velocity (derived from the GPS coordinates) and airspeed in a region of constant wind velocity, as long as the sailplane heading is changing during the measurement period. We have developed an algorithm to conduct this calculation [15] which is briefly summarised here.

First, the measured IAS is converted to TAS as described above. The ground velocity is calculated from the GPS coordinates. The flight path is then partitioned into cylindrical regions as shown in Fig. 6 with dimensions as shown. The horizontal wind velocity is assumed to be constant within each region and the wind velocity at the centre of each cylinder is calculated using data at the sample points along the flight path within each cylinder. The dimensions of the cylinders are chosen as a trade-off between the expected spatial rate of change of the wind velocity, the desired resolution of the wind velocity estimates, and the need for a sufficient number of data points within each cylinder.

The wind velocity estimate in each region is calculated as follows. Ground velocity and airspeed data at two sample points are selected and the two wind velocity solutions are calculated as described in the previous section. This is repeated for many pairs of sample points (typically about 100) within the cylinder and the pairs of solutions are subjected to a clustering analysis to find the set of solutions that are most consistent. The concept is described in the caption to Fig. 7. The pairs of data used and the clustering analysis is performed in such a way as to minimize the sensitivity to errors and the computational expense. The reader is referred to Ref. 15 for the details. The consistent wind velocity solutions within the cylinder then are averaged to provide the wind velocity estimate in that region. The analysis is repeated for each cylindrical region to give wind velocity estimates along the flight path.

The errors in the horizontal wind velocity estimates are assessed and minimized in various ways. First, we have shown [15] that the error in (each of the two) wind velocity estimates $|\Delta\mathbf{v}_w|$ derived from a pair of data is related to the error in the measured ground velocity $|\Delta\mathbf{v}_g|$ (or the error in the airspeed) by

$$|\Delta\mathbf{v}_w| = \frac{1}{\sin\Delta\theta}\,|\Delta\mathbf{v}_g| \tag{7}$$

where $\Delta\theta$ is the difference in sailplane heading at the two sample points. The "sensitivity" $(1/\cos\Delta\theta)$ is used to select the best sample points for analysis within each cylinder. This can be calculated without actually knowing the headings as described in Ref. 15. This shows that flight segments with almost constant heading do not provide good wind velocity estimates. Second, the clustering analysis partitions the wind velocity solutions into two sets, one which contains the correct solutions (set A) and one which contains the incorrect solutions (set B). The partitioning is based on the variance of the two sets, set A having a smaller variance (σ_A^2) than set B (σ_B^2). The larger the difference between these two variances, the more reliable is the partitioning and the more reliable the resulting wind velocity estimates. The reliability of the partitioning is, therefore, measured by the ratio $D = \sigma_B/\sigma_A$ and we use the final estimate from a cylinder only if $D > 3$. Third, the value of σ_A^2 is the variance of the wind velocity estimates in the cylinder. The final wind velocity estimate in the cylinder is the mean of these values, so that we can use $\sigma_A/2$ as

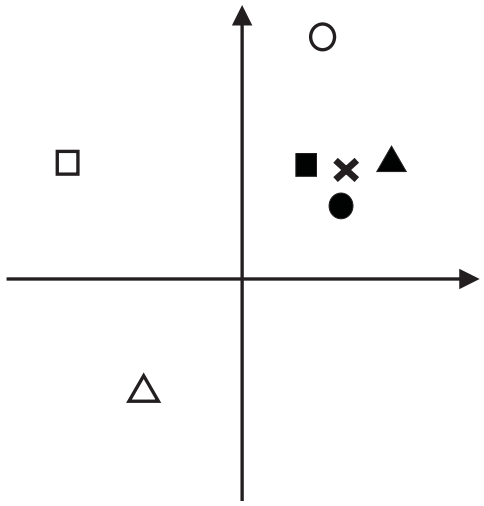

Figure 7 Illustration of the clustering analysis used to resolve the two-fold ambiguity from three pairs of data for the horizontal wind velocity estimate. The three kinds of symbol show the two solutions from each pair of data. The clustering analysis determines that the three filled symbols are the most consistent amongst the set of six estimates. The final wind velocity estimate is the centroid of those three and is denoted by the "x".

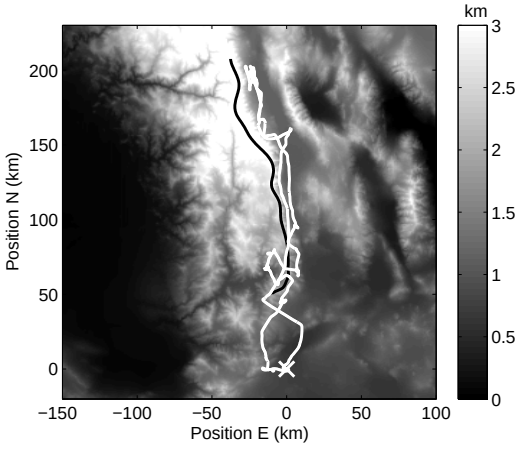

Figure 8 Topography map of the flight path region. The white line shows the flight path, and the black line denotes the ridge line, as described in the text. The cross denotes the takeoff point at California City. The coordinate origin is at the takeoff point.

a (conservative) estimate of the error in the final wind velocity estimate.

The vertical wind speed estimate is calculated straightforwardly as described in the previous section using Eq. 6. The sailplane vertical velocity is obtained by filtering and differentiating the GPS altitude. The sailplane sink rate is calculated from the flight polar and the indicated and true airspeeds as described above. The total energy correction is calculated by differentiating and low-pass filtering the airspeed so that rapid, unsustained fluctuations in the measured airspeed do not contribute to the correction. The bank angle is calculated and data with excessive bank are excluded as described above.

Application

The methods described above were applied to data from a flight in lee waves of the Sierra Nevada in southern California [15]. This is flight 39 of the Perlan Project [18]. The results are summarized here and the reader is referred to Ref. 15 for more details. The flight began at California City (35.2°N, 118.0°E, altitude 750 m) at 2140 UTC 24 April 2003 (1340 LT). The sailplane released from tow approximately 30 minutes after takeoff at an altitude of approximately 3500 m. The pilots were E. Enevoldson and S. Fossett. The flight lasted 4.8 h and proceeded along the Owens Valley to the east of the Sierra Nevada to Big Pine and returned to California City. The flight path is shown in Fig. 8. The flight altitude versus time is shown in Fig. 9. The maximum altitude was 13044 m.

The sailplane was a production Glaser-Dirks DG-505M (DG Flugzeugbau GmbH, Bruchsal, Germany) specially equipped for high-altitude flight. It was equipped with a modified Volkslogger GPS positioning system and pressure transducer (Garrecht Avionik GmbH, Bingen, Germany), a Borgelt B-50 airspeed indicator (Borgelt Instruments, Toowoomba, Aus-

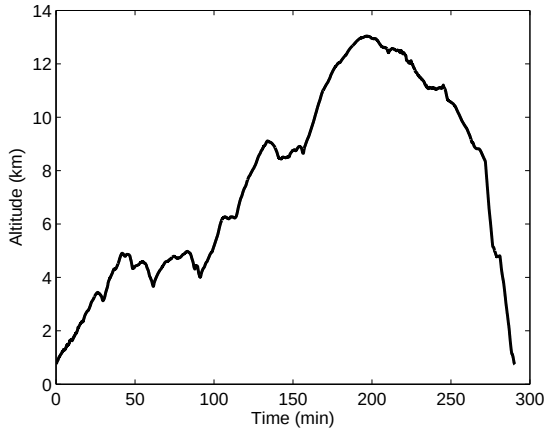

Figure 9 Sailplane altitude versus time after takeoff [15]

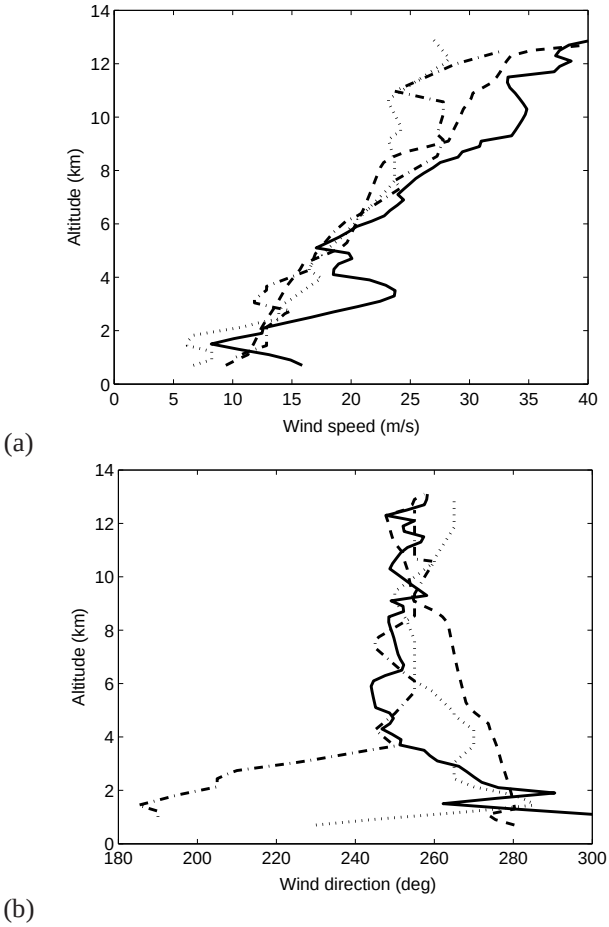

Figure 10 (a) Horizontal wind speed and (b) direction estimates vs altitude for the ascending (solid line) and the descending (dashed line) portions of the flight [15]. The radiosonde soundings at Edwards AFB (dotted line) and Desert Rock (dashed-dotted line) are also shown.

tralia), and a Platinum resistance temperature detector (RTD) outside air temperature probe. GPS fixes were obtained at 1 s intervals from the Volkslogger, and pressure recordings were made at 8 s intervals. Airspeed and temperature measurements were made at approximately 2.5 s intervals. The data were merged into a serial data stream and recorded on a custom datalogger. All data (except GPS fixes) were linearly interpolated onto the 1s GPS time stamps post flight. The sailplane flight polar was determined using a combination of the flight polar from the DG-505M flight manual and measurements made by comparison flights with a Duo Discus (Schempp-Hirth Flugzeugbau GmbH, Kirchheim unter Teck, Germany). Comparison flights were made at Omarama, New Zealand, in January 2003 with pilots E. Enevoldson and W. Walker. Several 5 minute runs were made at several airspeeds and differences in sink rate estimated. Run-to-run results were consistent and were averaged and used to validate the DG-505M polar.

The GPS coordinates and airspeed were low-pass filtered with a cutoff frequency of 1 Hz. The horizontal wind velocities were estimated as described in the previous section (using cylinder dimensions $r_{\text{region}} = 2$ km and $h_{\text{region}} = 100$ m) for the whole flight. These were collected into altitude bins 200 m thick and averaged, separately for the climbing and descending portions of the flight. The speed and direction are shown versus altitude in Fig. 10. Note the increasing wind speed with altitude and the fairly constant west-southwest direction. An example of the clustering of wind velocity solutions in one cylinder is shown in Fig. 11(a). The performance of the clustering analysis was assessed by calculating a histogram of the D values for the final wind velocity estimates which is shown in Fig. 11(b). These are all greater than 3 and 52% are greater than 10 indicating good separation of the two clusters. To assess the errors in the final wind velocity estimates, the distribution of σ_A is shown in Fig. 11(c). The values vary between 0.5 and 2.5 m/s, indicating errors in the wind velocity estimates between 0.3 and 1.3 m/s.

For comparison purposes, the wind speeds and directions recorded by radiosonde soundings at Edwards Air Force Base (AFB), Edwards, California (approximately 120 km south of the center of the flight path), at 1500 UTC 24 April 2003 and at Desert Rock, Mercury, Nevada (approximately 180 km east of the center of the flight path), at 0000 UTC 25 April 2003 are also shown in Fig. 10. These soundings are approximately 9 h before and at the time at the midpoint of the flight, respectively. Inspection of the figure shows quite good consistency between the estimated wind speeds and the soundings, given the different locations and times, and keeping in mind that the radiosondes are drifting east. The rms differences between the sailplane-derived estimates of the wind speed and direction and the average of the two soundings are 6 m s^{-1} and 8° (above 4000 m), respectively. In comparison, the rms differences between the two soundings are 3 m s^{-1} and 9°. Given the differing locations and times of the radiosonde soundings, the variation of the estimates is consistent with the errors estimated above.

The vertical wind speed along the flight path was estimated

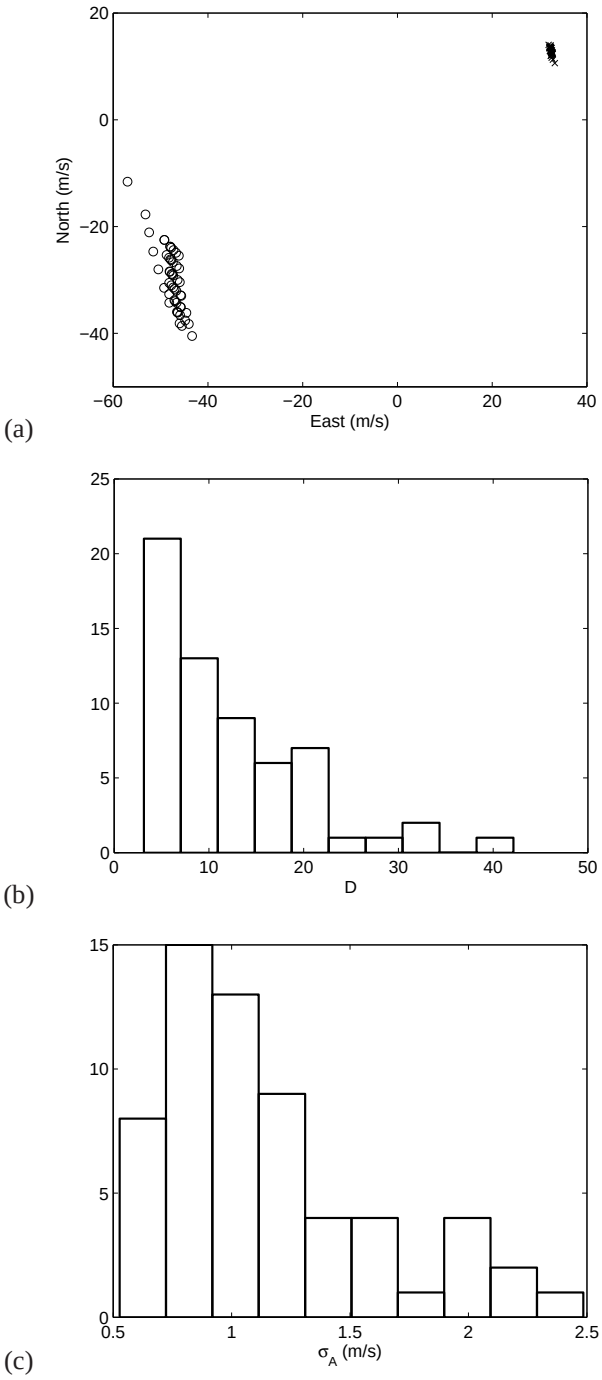

Figure 11 (a) An example of the clustering of wind velocity solutions in one of the cylinders. The correct solutions are shown by the crosses and the incorrect solutions by the circles. (b) Histogram of D values to assess the reliability of the clustering. (c) Histogram of σ_A indicating the accuracy of the wind velocity estimates.

as described in the previous section. The rate of change of airspeed was calculated by finite differences over a time interval of 8 s. This window length provided a good compromise to remove transient airspeed changes but include more sustained changes that affect the sailplane vertical speed. The vertical wind speed estimates were calculated every 1 s and low-pass filtered with a cutoff frequency of 0.2 Hz. The importance of the total energy correction is illustrated in Fig. 12 which shows the airspeed and the corresponding sailplane vertical speed and the derived vertical wind speed versus time for a portion of the flight. The figure shows that large excursions in the measured sailplane vertical speed due to rapid changes in the airspeed are removed when computing the vertical wind speed with total energy correction as described above.

The wave structure is in principle fixed relative to the terrain for short periods. For the northern part of this flight, the dominant terrain is the eastern ridge of the mountain range, running

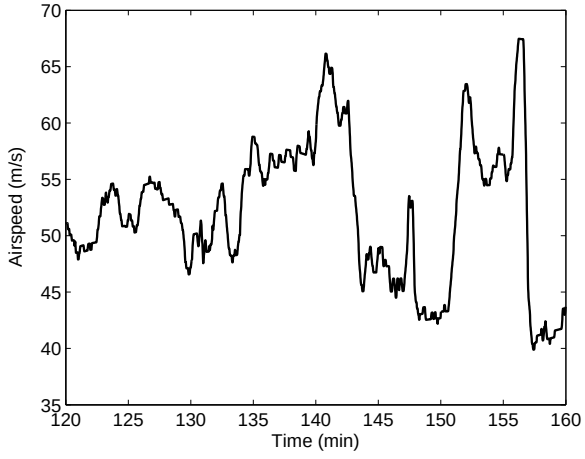

(a)

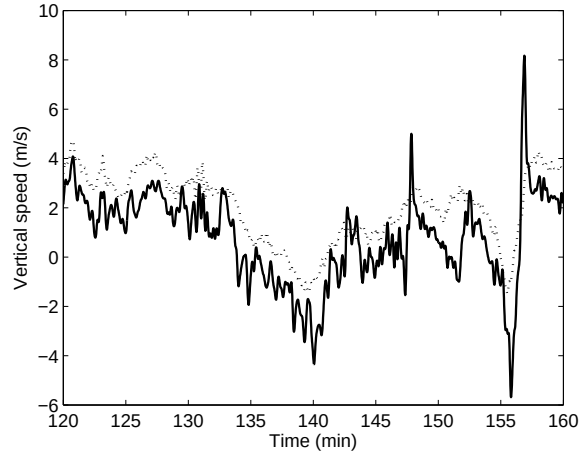

(b)

Figure 12 Flight segment between 7200 s and 9600 s showing (a) the airspeed and (b) the sailplane vertical ground speed (solid line) and the vertical wind speed (dotted line), calculated as described in the text.

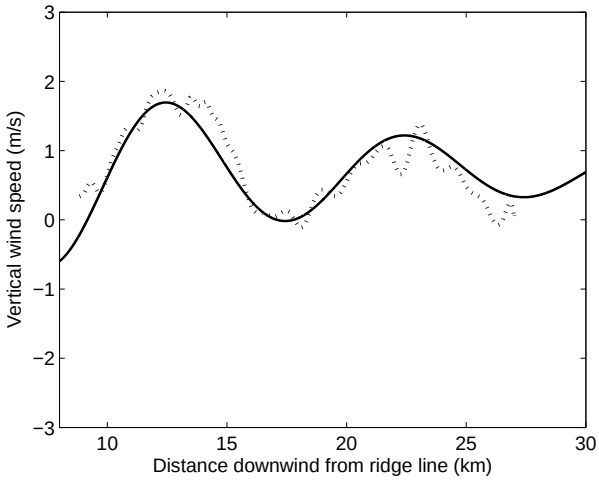

Figure 13 Vertical wind speed estimates versus distance downwind from a short segment of the ridge line as described in the text (dots) [15] The solid line shows a fitted exponentially damped sinusoid.

north-northwest to south-southeast, to the west of the flight path. We, therefore, take as a terrain reference the center line of this ridge, which we refer to as the "ridge line." Points at maximum altitude along this ridge were located manually from the topography, and the ridge line was determined by spline interpolation. The resulting ridge line is shown as the black line in Fig. 8.

The wave structure is most clearly evident in a plot of the vertical wind speed versus distance downwind from a particular point on the ridge line and at a fixed altitude. The streamlines in such a plot are expected to approximately follow an exponentially damped sinusoid, and for a constant horizontal wind speed, the vertical wind speed is also an exponentially damped sinusoid that is phase shifted relative to the streamlines. A primarily downwind segment of the flight path of significant length is a 4-min segment near the maximum altitude of the flight, south of Lone Pine. This flight segment extends approximately 20 km downwind, the altitude varies between 12360 and 12500 m, and it is downwind of a 6-km section of the ridge line. The estimated vertical wind speed versus distance downwind from the ridge line for this portion of the flight is shown in Fig. 13. Inspection of the figure shows a wave structure, and a least-squares fit of an exponentially damped sinusoid to the data is also shown in Fig. 13. The fit is quite good (correlation coefficient = 0.9) and gives a wavelength of 10 km. The mean vertical wind speed estimate in this region is offset from zero by approximately 0.7 m/s. This is not unusual for short distances of the order of 1–2 wavelengths (see for example Ref. 12). A plot of the Scorer parameter [19] versus altitude above 5000 m calculated from the average recorded lapse rate and the derived horizontal wind speeds is shown in Fig. 14. The decreasing Scorer parameter with altitude indicates ideal conditions for the development of lee waves [19].

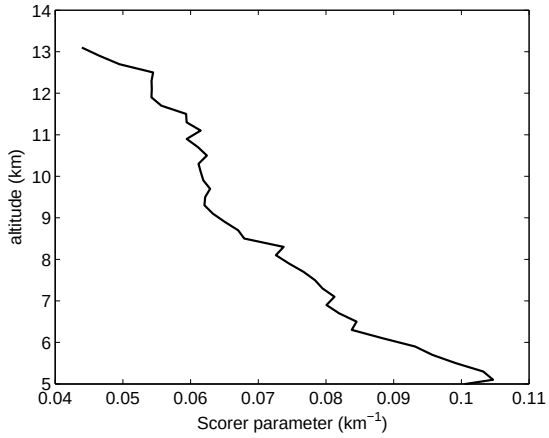

Figure 14 Scorer parameter versus altitude calculated from the average recorded lapse rate and the derived horizontal wind speed above 5000 m.

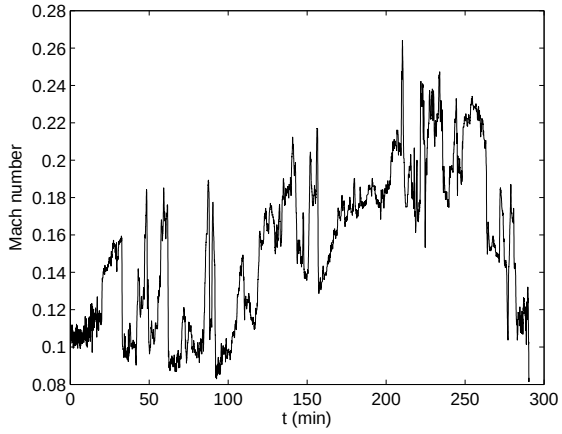

Figure 15 Mach number versus flight time.

Discussion

Sailplanes are potentially useful as a meteorological instrument. This is due to their simple and well-characterised flight characteristics, and to their often being flown in interesting meteorological conditions. A highly instrumented sailplane can be used to collect comprehensive data, but useful information also can be obtained from a lightly instrumented sailplane. The slowly varying nature of the horizontal wind velocity in mountain waves allows good estimates of the 3D wind field to be obtained from only logged GPS and airspeed data, and an algorithm to effect this calculation has been described. This provides an interesting and potentially useful way of measuring wind fields in mountain waves, which are otherwise not easily accessible. Implementation of the algorithm and application to a sailplane wave flight show that it is effective, with reasonably good agreement between derived horizontal wind speeds and those from radiosonde soundings, and with derived vertical wind speeds that are overall consistent with expectations. More comprehensive information could be obtained by a skilled pilot systematically exploring a wave system with this objective. There is also the possibility of pooling data from a number of sailplanes flying in the same region to improve coverage and accuracy.

Since sailplanes do not generally carry equipment that logs airspeed, it is of interest to consider the potential for estimating the wind velocity without the benefit of airspeed data. Standard flight records log only position and time, so the question becomes how much information can be obtained on the wind velocity using only this data? This would offer the possibility of using routine glider flights as "sensors of opportunity." The problem is highly undetermined in general, even if the wind velocity is constant in an appropriate measurement interval. However, incorporation of other information may allow a solution to be obtained. For example, even if the airspeed is not measured, it is known that it is between the stall speed and the maximum airspeed (v_{NE}), and this provides limits on the possible wind velocities. Appropriate incorporation of this and other *a priori* information may impose sufficient constraints to make accurate wind velocity estimates. Note that once the wind velocity is estimated, the airspeed can be calculated and the necessary corrections described above made to obtain the vertical wind speed. The potential of this approach is worthy of further investigation.

Finally, it is interesting to consider the effect of approaching the speed of sound for high altitude sailplane flights. The Mach number versus time for this flight is shown in Fig. 15. Note that the Mach number reaches 0.26 at the maximum altitude of 13000 m. For higher altitude flights the IAS operating region will begin to be limited by the Mach number.

Acknowledgements

We are grateful to the NZ TEC for award of Top Achiever Doctoral scholarship to NZ, the Electrical and Computer Engineering Department at the UC for a research grant, and NASA for support. Perlan Project flights are supported by the Steve Fossett Challenges.

References

[1] R. S. Scorer. *Dynamics of Meteorology and Climate*. Wiley, New York, 1997.

[2] D. Durran. *Mountain waves and down slope winds. Atmospheric processes over complex terrain.* Number 45 in Meteor. Monogr. Amer. Meteor. Soc., 1990. pp. 59–82.

[3] K. Sato. Vertical wind distrubances in the troposphere and lower stratosphere observed by the MU radar. *J. Atmos. Sci.*, 47:2803–2817, 1990.

[4] J. C. Bird et al. Observations of ozone structure in the artctic polar vortex. *J. Geophys. Res.*, 102:10785–10800, 1997.

[5] J. R. Holton. The influence of gravity wave breaking on the general circulation of the middle atmosphere. *J. Atmos. Sci.*, 40:186–201, 1983.

[6] S. B. Vosper, P. F. Sheridan, and A. R. Brown. Flow separation and rotor information beneath two-dimensional trapped lee waves. *Quart. J. Roy. Meteorol. Soc.*, 132, 2006.

[7] J. L. Green, K. S. Gage, and T. E. V. Zandt. Atmospheric measurements by VHF pulsed doppler radar. *IEEE Trans. Geosci. Electron.*, 17:262–280, 1979.

[8] D. Khelif, S. P. Burns, and C. A. Friehe. Improved wind measurements on research aircraft. *J. Atmos. Oceanic Technol.*, 16:860–875, 1999.

[9] R. Wood, I. M. Stromberg, P. R. Jonas, and C. S. Mill. Analysis of an air motion system on light aircraft for boundary layer research. *J. Atmos. Oceanic. Technol.*, 14:960–968, 1997.

[10] R. F. Whelan. *Exploring the Monster: Mountain Lee Waves: The Aerial Elevator*. Wind Canyon Books, Niceville, 2000.

[11] S. Myschik and G. Sachs. Wind measurement system using miniaturized navigation sensors for light aircraft and sailplanes. *Technical Soaring*, 33(1):2–6, 2009.

[12] C. Lindemann, R. Heise, and W. Herold. Lee waves in the Andes region, mountain wave project (MWP) of OSTIV. *Technical Soaring*, 32:93–96, 2008.

[13] J. Dummann. A report on glider pilot activities to document lee wave events in northern germany and their aims. *Technical Soaring*, 33:109–116, 2009.

[14] R. F. Hertenstein and C. L. Martin. Observations of internal rotor structure using an instrumented sailplane. *Technical Soaring*, 32(4):108–114, 2008.

[15] R. P. Millane et al. Estimating wind velocities in mountain lee waves using sailplane flight data. *J. Atmospheric Oceanic Technol.*, 27:147–158, 2010.

[16] W. M. Olson. Aircraft performance flight testing. Technical Report AFFTC-TIH-99-02, United States Air Force, Air Force Flight Test Center, Edwards AFB, CA, 2002.

[17] A. Welch, L. Welch, and F. Irving. *New Soaring Pilot*. John Murray, London, 3rd edition, 1977. pp. 238ff.

[18] E. J. Carter, E. H. Teets, and S. N. Goates. The Perlan project: New Zealand flights, meteorological support & modeling. In *Preprints, 19th Conf. on IIPS, Long Beach, CA*. Amer. Meteor. Soc., 2003. Available online at http://ams.confex.com/ams/pdfpapers/56190.pdf.

[19] R. S Scorer. Theory of waves in the lee of mountains. *Quart. J. Roy. Meteor. Soc.*, 75:41–56, 1949.